

Article

A Physical Model Test of Coal-Mining-Induced Deformation Mechanisms in a Canal

Renwei Ding, Ye Tian , Handong Liu, Tong Jiang , Huaichang Yu and Dongdong Li *

College of Geosciences and Engineering, North China University of Water Resources and Electric Power, Zhengzhou 450045, China; dingrenwei@ncwu.edu.cn (R.D.); z202210020293@stu.ncwu.edu.cn (Y.T.); liuhandong@ncwu.edu.cn (H.L.); jiangtong@ncwu.edu.cn (T.J.); yuhuaichang@ncwu.edu.cn (H.Y.)

* Correspondence: lidongdong@ncwu.edu.cn

Abstract: The route of the South-to-North Water Diversion channel strides across part of the coal mine goaf in Yuzhou County, Henan Province, China, and long-term deformation due to coal seam recovery poses a threat to the safe operation of the main canal. Therefore, the study of the deformation mechanisms induced by coal seam recovery is of great significance to the canal's safe operation, as well as to deformation monitoring and to the development of early warnings. The geologic model was established based on the geological engineering conditions of the Yuzhou Gongmao mining area, spanning the main canal of the South-to-North Water Diversion Project; then, the physical model test was carried out according to similar theories. The deformation characteristics of the rock overlay and the channel above the goaf were analyzed, and failure criteria for overburdened rock and the channel were proposed. The results showed that horizontal fissures were gradually observed in the overlying rock as the coal mining progressed, extending and widening. When the goaf was excavated to 76 cm, the overlying rock body suddenly collapsed as a whole, and the channel collapsed and was destroyed. During the formation of the goaf, there was a critical span ratio (R): When the height-to-span ratio was greater than 0.039, the collapse of overlying rock occurred only within a certain range above the goaf. When the height-to-span ratio was less than 0.039, the overlying rock body collapsed in a wide area, and the soil on both sides of the channel collapsed to the center of the channel, presenting a "V" glyph collapse. The sediment in the center of the channel measured 22 mm, and there were multiple tensile cracks on both sides of the embankment, with a width of 5–10 mm. The vertical deformation of the channel went through three stages, namely, the initial deformation stage, the deceleration deformation stage, and the stability stage. This study can provide scientific guidance for early warnings of channel deformation and safe operation across the goaf.

Keywords: South-to-North Water Diversion Project; coal mining; deformation mechanism; height-to-span ratio



Academic Editor: Douglas O'Shaughnessy

Received: 15 December 2024

Revised: 10 January 2025

Accepted: 17 January 2025

Published: 29 January 2025

Citation: Ding, R.; Tian, Y.; Liu, H.; Jiang, T.; Yu, H.; Li, D. A Physical Model Test of Coal-Mining-Induced Deformation Mechanisms in a Canal. *Appl. Sci.* **2025**, *15*, 1384. <https://doi.org/10.3390/app15031384>

Copyright: © 2025 by the authors. Licensee MDPI, Basel, Switzerland. This article is an open access article distributed under the terms and conditions of the Creative Commons Attribution (CC BY) license (<https://creativecommons.org/licenses/by/4.0/>).

1. Introduction

The middle route of the South-to-North Water Diversion Project is a water transfer project from the Danjiangkou Reservoir in the upper reaches of the Han River, a tributary of the Yangtze River that flows through the Yangtze River Basin and the Huaihe River Basin to the Tuancheng Lake of the Summer Palace in Beijing. The middle route of the South-to-North Water Diversion Project spans the provinces of Henan and Hebei as well as the Tianjin and Beijing municipalities, focusing on solving the water shortage problem of these regions and the production, residential, industrial, and agricultural water use of the large and medium-sized cities along its route. The total water supply area is 155,000 km²,

and the total length of the main water transmission channel is 1432 km. The route of the South-to-North Water Diversion channel strides across part of the coal mine goaf in Yuzhou County, Henan Province. When the long-term deformation and coal seam recovery deformation are serious, the overburdened deformation could become unstable, which will affect the stability of buildings and pose a threat to the safe operation of the main canal; therefore, this study examined the effect of coal seam recovery deformation mechanisms on the safe operation of channels and deformation monitoring and early warning systems.

Currently, scholars have conducted a great deal of research on surface subsidence, rock layer movement, and the destruction of upper surface buildings (structures) caused by coal mining, focusing on the deformation law of the surface and deep parts of the goaf; site subsidence monitoring in the goaf; ground catastrophe mechanisms, prevention, and control; goaf management technologies; and other aspects [1–11]. Commonly used goaf stability evaluation methods mainly include physical model tests, nonlinear evaluations, numerical simulations, etc. The stability analysis of Jinjitan coal mine was conducted by Liu et al. [12], combining field investigations and deformation monitoring with Brillouin optical time domain reflectometry (BOTDR). Castellanza et al. [13] analyzed the attenuation of relative humidity on the strength of the ore column. Auvray et al. [14] made stress measurements for the ore column at different times, and studied the stability of the goaf by establishing the relationship between the weathering thickness and the ore column time. In coal seam mining, Tan et al. [7] studied the structure of stope cover rock and the law of cover rock fissure development. Wang et al. [15] analyzed the relationship between the mechanical state of the roof and the total area of the column and the impact of weathering and peeling on the bearing area of the column, obtaining the influence of the bearing area on the stability of the roof.

Through a model test, Han et al. [16] analyzed the influence of goaf roof fracture movement on disturbances along empty lanes and obtained the limit span of the key rock layer and the load filling in the wall, proposing control technologies to improve the stability of the surrounding rock along empty lanes. Hanson et al. [17] studied the rupture mechanism of closed cracks under cyclic loading and unloading conditions by 3D numerical simulations. Bäckblom et al. [18] proposed a functional relationship between the area of damage formed by excavation and the rock mass strength, initial stress field, and geometric form of the excavation surface, conducted many statistical analyses based on the Hoek–Brown criterion, and summarized the empirical rule of predicting the depth of destruction. Based on the risk approach index of Zhang et al. [19], the stability of underground rock engineering has been evaluated and analyzed. Detournay et al. [20] summarized the possible pattern and mechanism of destruction of unsupported circular underground cavities. Osgoui et al. [21] studied the action mechanism of rock surrounding roadways after grouting and reinforcement and analyzed the process of plastic deformation on surrounding rock. Guo et al. [22] proposed a prediction method for the solid filling of coal mining-caused subsidence to predict surface subsidence.

Large engineering construction projects usually bypass some complex geological engineering conditions or areas. However, with growing national strategic development needs, some projects have to go through these areas. The safety of the construction project and its normal operations need to be ensured. There are some goafs in the way of the middle route of the South-to-North Water Diversion project. The Henan and Hebei Provinces have 11 coal mines, and the Yuzhou goaf section passes through five coal mine goafs. To date, there have been many examples of road and railway engineering studies on goaf crossing at home and abroad, while few studies on the goaf under the water transmission channel have been presented [23,24], especially on the deformation and damage caused by the excavation of the goaf.

Mining has been carried out in the Gongmao mining area in Yuzhou for a long time; due to the large-scale mining of the coal seam, the formation loss and stress field change, the overlying rock body collapses, fractures and deformations occur, and a large number of cracks and moving basins appear on the surface, with crack widths of 2–15 cm, strike lengths of 200 m, and depths of 0.5–5 m. The coexistence of large and small coal mines in this area and the non-standard mining led to complex surface movement and deformation in the goaf, and there is no regularity. This paper uses the Gongmao mining area as a prototype, from which a geo-mechanical model was established; then, a physical model test was carried out according to similar theories, resulting in the determination of the failure and destruction characteristics of the rock overlay and channel due to recovery and the establishment of discrimination criteria for overlying rock and channel instability deformation.

2. Geological Setting

The main canal of the South-to-North Water Diversion Project in Yuzhou County stretches across an area with low mountains and hills with a monoclinic mountain terrain, low in the east and high in the west, with an elevation of 100–700 m. The passing section of the channel is in the transition zone between the flood accumulation skirt around Sanfeng Mountain and the plain. The terrain is relatively gentle, and the ground elevation is 123–145 m. The landform of the goaf section is shown in Figure 1.

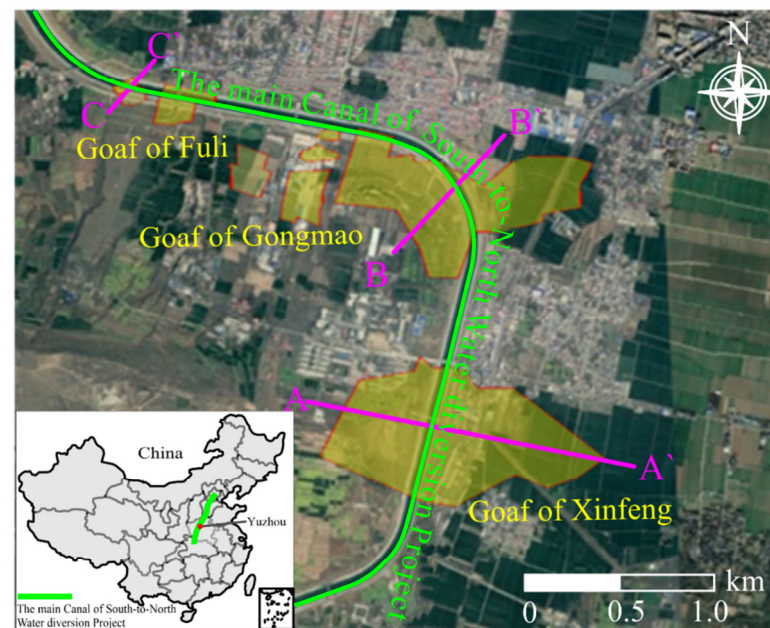


Figure 1. Mining area spanning the main canal of the South-to-North Water Diversion Project in Yuzhou County.

The surface was covered by the quaternary strata, while the underlying strata are mainly the Permian Middle System Shihezi Formation (P_2sh), the Pingdingshan Formation (P_2p), and the Carboniferous Upper System Taiyuan Formation (C_3t). The dip direction of the formation is approximately 195° , and the dip angle is 10 to 20° . According to the exploration data, the strata of the Taiyuan Formation (C_3t) of the Upper Carboniferous System in the area are mainly limestone, with a thickness of 55–124 m and an average thickness of 70 m. The Permian Middle System Shihezi group (P_2sh) is mainly composed of gray and green mudstone, sandy mudstone, and gray and white sandstone, mixed with purple-red porphy shale, carbon shale, and coal seam. The rock combination has strong regularity and obvious sedimentary rotation, with a thickness of 520–561 m and an average

thickness of 536 m. The Permian Pingdingshan Formation (P_2p) is mainly gray-white feldspar quartz sandstone, with silicate cementation, with a thickness of 58–95 m and an average thickness of 80 m. The coal seam and the goaf are mainly located in the sandstone and mudstone layer of the Permian Shihezi group (Figure 2).

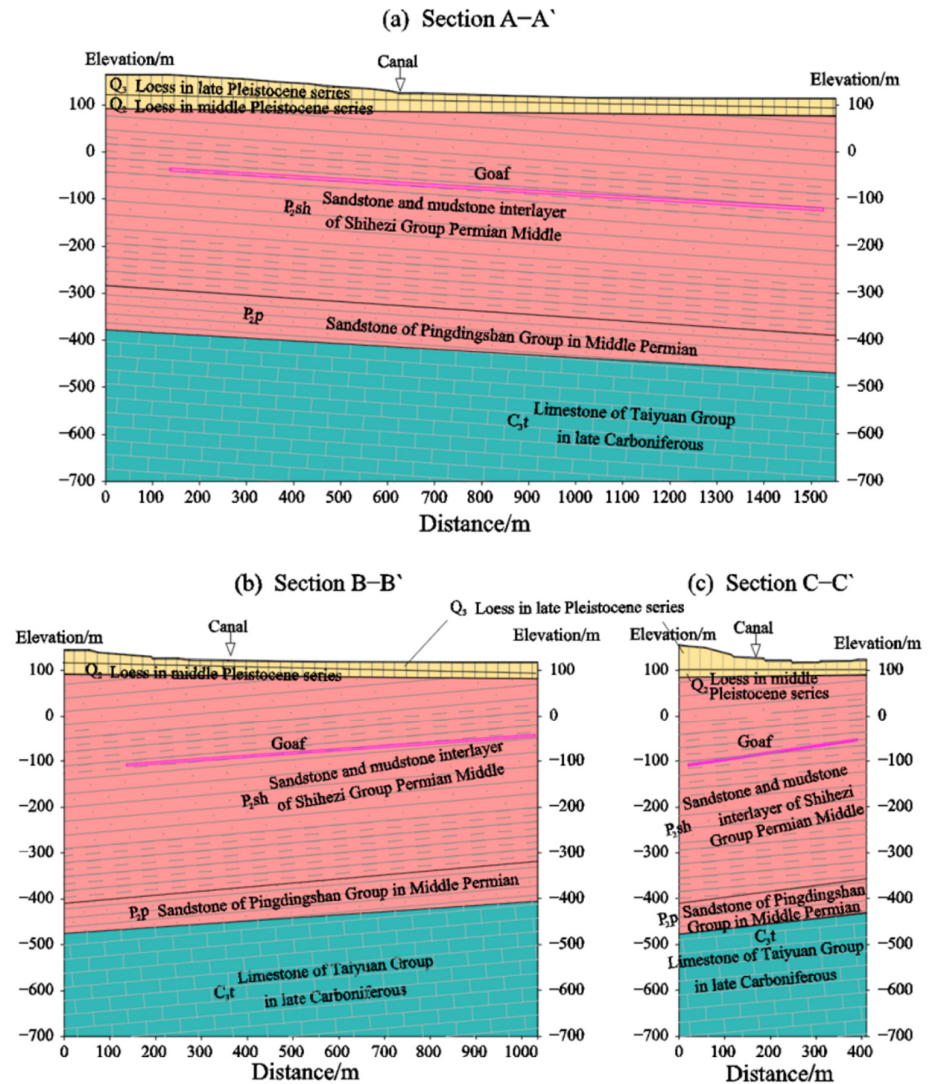


Figure 2. Engineering geological section of the goaf under the canal.

The stratum direction of the Yuzhou coal mine area is east–west, and the mining area formed a multiple strip distribution in the goaf area, which is the same as that in the coal mine area. The goaf area is formed by the irregular mining of the local small collectives. The roof of the goaf is mostly supported by simple devices or maintained by the stability of the goaf itself. The channel mainly spans three goaf areas, and the scale of the goaf varies greatly. The distribution range of the goaf below the channel is shown in Figure 1.

3. Physical Model Test

3.1. Materials

According to the stratigraphic distribution in the Gongmao mining area, the overlying rock mass and quaternary overlayer can be generalized, among which the overlying rock body has been grouted and strengthened during the construction of the middle route of the South-to-North Water Diversion Project. In this test, the bulk weight similarity constant of the grouted rock mass was determined to be 1. Combined with the relevant mechanical

parameters of the grouted rock mass in the research area, and drawing on the existing research experience, gypsum, fine sand, barite powder, and alcohol were selected as the raw materials to help produce representative materials. After the representative materials are determined, a ratio test was carried out according to the mechanical parameters of the overlying rock body. The specimens were made by different proportioning methods, and the physical and mechanical parameters of the specimens were determined through correlation tests; the test results were compared with the relevant parameters of the overlying rock body, and the most reasonable mix ratio of the representative materials was selected (Tables 1 and 2). The loess soil in the field was taken as the test material for the canal, and its related mechanical parameters remained unchanged.

Table 1. Ratio of raw material for rock mass (mass ratio).

Raw Material	Fine Sand	Barite Powder	Gypsum	Alcohol
Ratio	0.59	0.22	0.13	0.06

Table 2. Physical and mechanical parameters of overburdened rock.

Parameters	γ (kN/m ³)	E /GPa	μ	c /MPa	ϕ /(°)
Grouted rock mass	21	1.5	0.28	0.6	31
Representative materials	21	0.015	0.28	0.006	31
Similarity ratio	1	100	1	100	1

3.2. Experimental Setup

Based on the engineering geological conditions of the Gongmao mining area in Yuzhou in the middle route of the South-to-North Water Diversion Project, the geometric similarity ratio of the physical model test was set as 1:100, considering the test conditions and similarity theories. Firstly, the height of the overlying rock body and the soil mass at the bottom of the canal in the tested goaf were determined according to the engineering geological profile of the mining area; then, a steel frame model box was established, with a length, width, and height of 1400 mm, 400 mm, and 1400 mm, respectively. The front and rear facades of the model box were made of 10 steel plates which were 1400 mm long and 140 mm wide, respectively. Secondly, the rock mass was filled with the representative materials. The rock mass filling was divided into 7 layers; each layer of filler was 7 cm thick, and each layer of tamping was divided into 4 steps: paving leveling, initial tamping, heavy tamping, and leveling. In order for the two layers to be well cemented, the upper surface needed to be brushed. Finally, the loess soil layer was filled with raw materials, in line with the above steps, and the model at this point is shown in Figure 3. During the compaction of experiment materials in the test box, a steel plate was fixed on the side facade using bolts, which was replaced with a tempered glass plate of the same size before the test began, so as to observe and record the deformation and damage of the covered rock mass during the test.

The model test mainly studies the deformation characteristics of the rock mass and the channel. Therefore, the deformation process of the overlying rock mass and the channel over the goaf was recorded. In order to measure the deformation characteristics of the upper rock mass, a square grid, 10 cm long and 7 cm wide, respectively, was drawn on the side facade. The deformation process of the side facade and the cross point of the grid line were regularly recorded by the 3D laser scanner. In order to measure the deformation process of the channel and the bank slope, a self-made deep displacement meter and a

displacement sensor were acquired, and the data acquisition frequency was 1 Hz. Vertical deformation measuring points of the same depth were arranged on the same side of the channel, monitoring points of different depths at the center and on the other side of the channel (Figures 3 and 4).

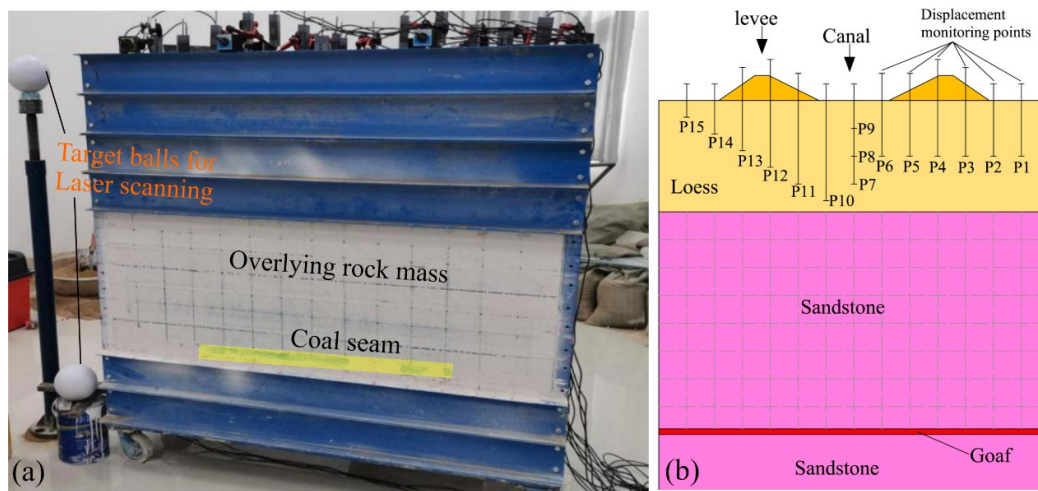


Figure 3. Experimental setup. (a) Test equipment; (b) test system.

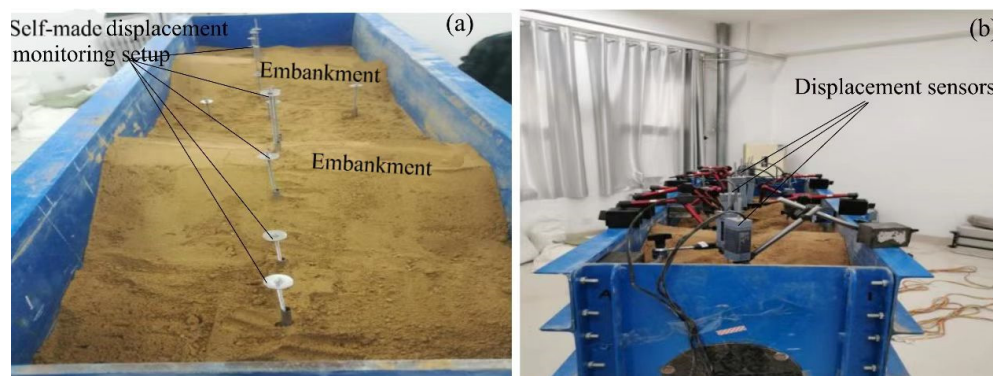


Figure 4. Layout of soil displacement monitoring points. (a) Self-made displacement monitoring setup; (b) displacement sensors.

4. Results

This test mainly studies the influence of the goaf recovery process below the channel on the deformation characteristics of the channel and the overlying rock mass. After the test began, excavation was performed directly at the bottom of the canal to simulate the recovery process. To facilitate the implementation of the excavation process, the foam plate was replaced during the model fabrication process. The first excavation length was 20 cm long to simulate the existing goaf. In the following excavation process, 4 cm was removed from each side each time a further excavation was conducted, resulting in a total length of 8 cm. After each excavation, the next excavation was not conducted until the deformation of the overburdened rock was stable. After eight excavations, the overlying rock body peaked, and the channel center collapsed. The following were the detailed deformation characteristics of the overlying rock mass and the channel.

4.1. Deformation Characteristics of Overlying Rock Mass

Figure 5 shows the deformation and destruction characteristics of the overlying rock mass over the goaf during the recovery process. The first excavation of 20 cm from the center to both sides was conducted to simulate the formation process of the existing goaf.

After the completion of the first excavation, the upper rock mass was in a stable state, no cracks appeared, there was no rock mass falling at the top of the goaf, and no obvious horizontal and vertical deformation was observed in the upper rock mass. The second excavation length was 8 cm, resulting in a horizontal crack with a length of 6 cm about 3.5 cm over the goaf. About 8 h after the excavation, another horizontal crack about 10 cm long and about 6.5 cm above the roof was observed, and the first crack extended to 14 cm. The upper rock mass was in a critical stable state without collapse. After the third excavation of 8 cm, a horizontal crack about 16 cm long appeared about 10.5 cm above the headplate. At this time, the first crack extended to 27 cm, with a width of about 1 mm, and the second horizontal crack extended to 19 cm.

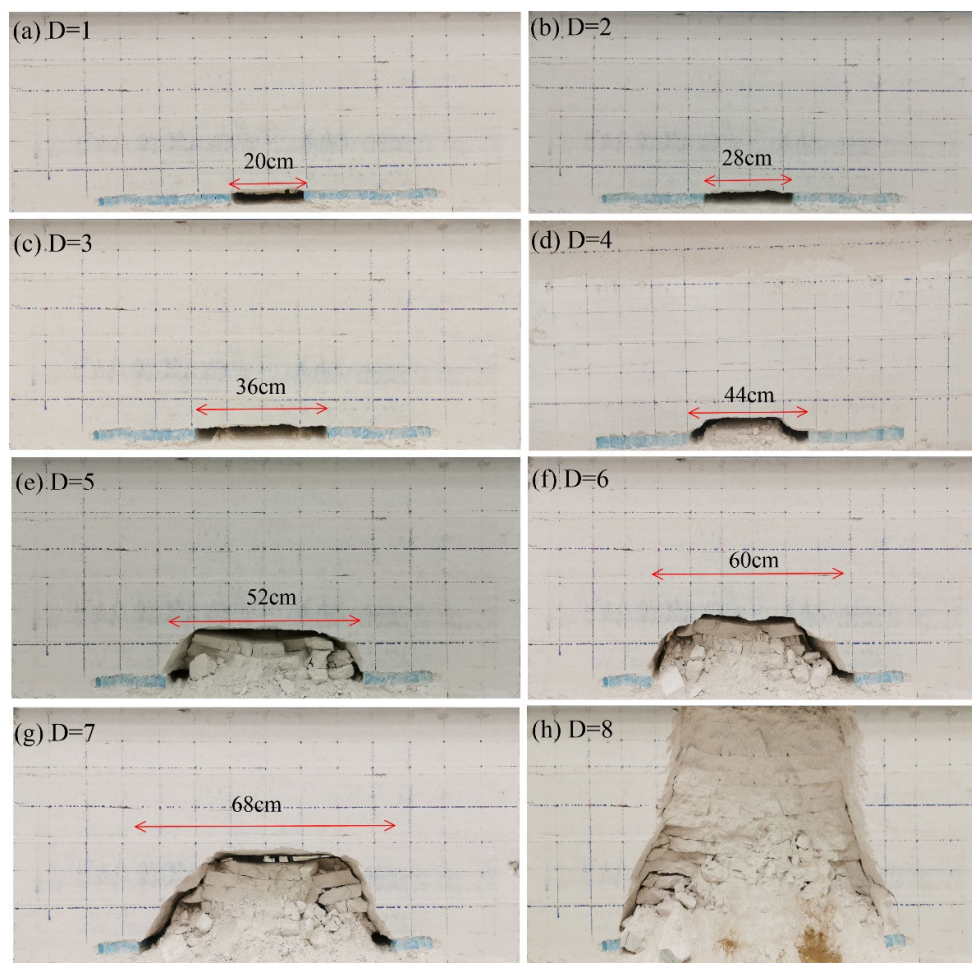


Figure 5. Failure process of overburdened rock during coal seam recovery. (a) D = 1; (b) D = 2; (c) D = 3; (d) D = 4; (e) D = 5; (f) D = 6; (g) D = 7; (h) D = 8.

After the fourth excavation, the first collapse was observed approximately 3.5 cm above the roof, with a length of about 28 cm; the horizontal crack 6.5 cm above the roof extended to 28 cm and the crack 10.5 cm above the roof to 22 cm. After completion of the fifth excavation, a second collapse of the rock mass occurred approximately 12 cm above the roof of the goaf, with a length of about 34 cm; a new horizontal crack, about 6 cm long, appeared about 14 cm above the roof and another one, about 10 cm long, 17 cm above the roof. After the sixth excavation, a third collapse occurred approximately 15 cm above the roof, with a length of about 36 cm, and three new cracks, about 28 cm, 13 cm, and 12 cm long, respectively, were observed about 20 cm, 22 cm, and 25 cm above the roof. After the seventh excavation, a fourth collapse occurred approximately 19 cm above the roof. The width of the collapse band was about 38 cm, the crack at 25 cm above the roof extended

to 30 cm, and a horizontal crack, about 9 cm long, appeared 30 cm above the roof. After the eighth excavation, the rock mass completely collapsed, forming a collapse zone with a height of 50 cm, top width of 53 cm, and bottom width of 76 cm. The degree of deformation and destruction of the upper covered rock mass in the goaf increased gradually with the mining progress in the goaf. The deformation and destruction process could be generally summarized as loose unloading, horizontal fracture extension, and roof collapse.

Figure 6 shows a cloud map of the overall deformation distribution of the upper covered rock mass in the mining process obtained based on 3D laser scanning technology, which can reveal the influence of the mining process on the deformation range and deformation value of the covered rock. After the first and second excavations, the height-to-span ratio was 0.15 and 0.107, respectively, with only a little deformation in the excavated area, and the deformation of the upper covered rock was small. After the third time, the height-to-span ratio was 0.083, and the rock mass above the excavation surface began to move. After the fourth excavation, the collapse height was about twice the excavation height with a height-to-span ratio of about 0.068. After the fifth excavation, the collapse height was about thrice the excavation height, with a height-to-span ratio of about 0.058. The collapse height was about fourfold taller than the excavation height, with a height-to-span ratio of about 0.05 and 0.044 for the sixth and seventh excavations, respectively. However, after the eighth excavation, the height-to-span ratio decreased to 0.039, and overall collapse occurred throughout the entire rock. Therefore, from the analysis of the whole test process, in terms of the relationship between the height of the excavation area (H) and the rock collapse span (D), there was a critical height ratio (R) in the goaf excavation. When the height ratio is greater than the critical value, collapse only occurs within a certain height range, and the overburden is stable as a whole. With the progress of excavation, when the height ratio reaches and gradually decreases beyond the critical value, the rock mass above the goaf collapses, the deformation increases sharply, and the collapsed area is trapezoidal. Subsequently, the height ratio continues to decrease, and the collapse area and deformation increase slightly.

Figure 7 shows the vertical displacement curves of characteristic points at different heights above the excavation surface obtained by 3D laser scanning technology. The error of the displacement was less than 0.1 mm. “ $D = 1$ ” in the figure represents the vertical displacement curve after the first excavation, and so on. Figure 7a–c represent the process of the vertical displacement change in characteristic points 0.1 m, 0.2 m, and 0.3 m, respectively, apart from the top height of the excavation surface. On the whole, the vertical deformation of the rock covering above the goaf had obvious mutations. After the completion of the first seven excavations, the deformation of the rock covering was small, and the closer the deformation to the excavation surface, the more obvious the vertical deformation. The maximum deformation was 3.7 mm, and the further the deformation was from the excavation surface, the smaller the deformation was. After the eighth excavation was completed, the covered rock deformation rose sharply (Figure 7d), showing an obvious collapse deformation. In addition, the vertical deformation amount of the covered rock in the mining center of the same horizontal surface was significantly greater than that on both sides, showing the characteristics of a large middle size and a gradual decrease at both ends. In the vertical direction, the vertical deformation decreased slightly as the distance from the excavation surface increased.

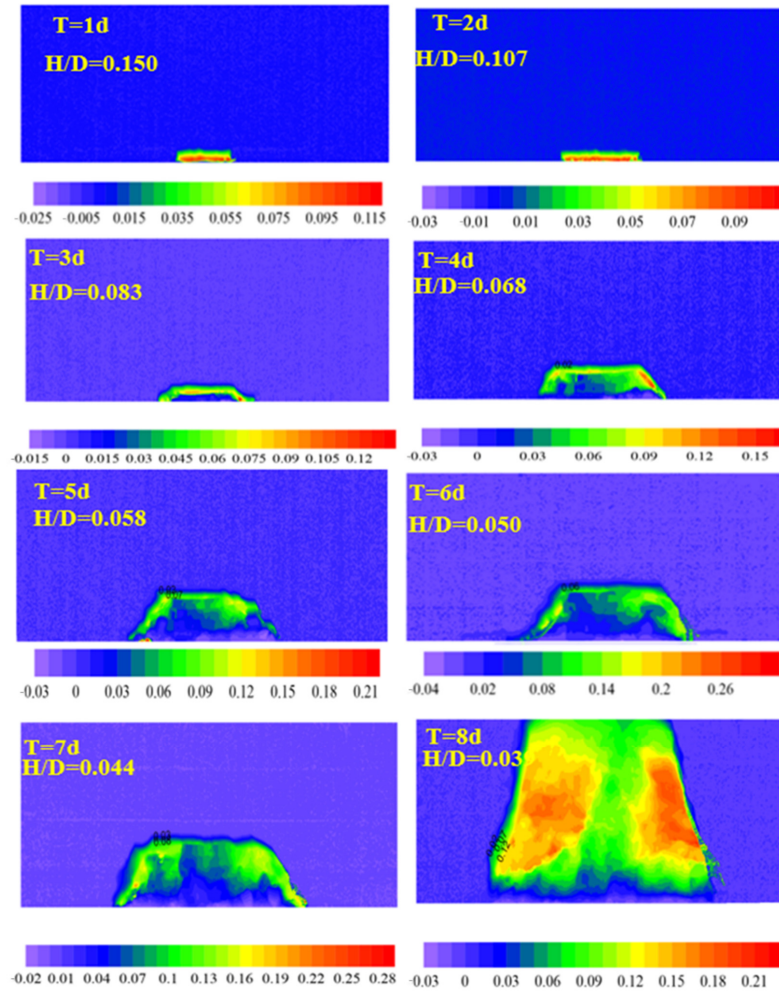


Figure 6. Deformation cloud map of overlying strata during mining (unit: m).

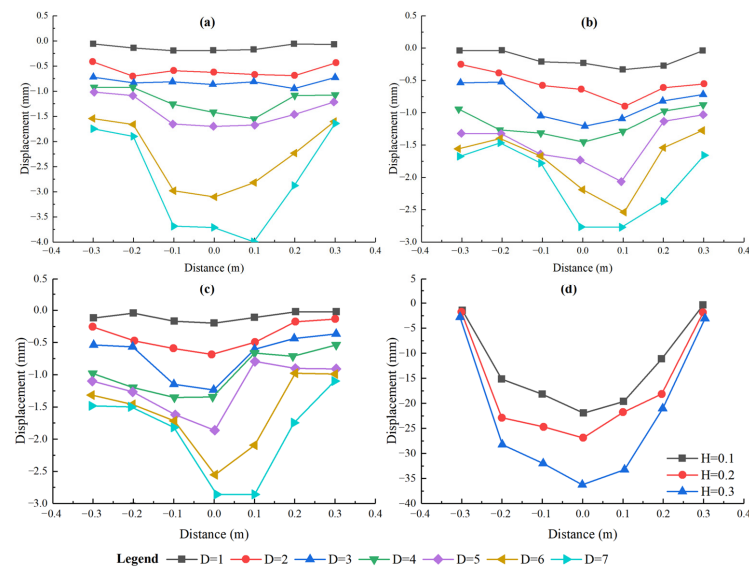


Figure 7. Vertical distance of monitoring points on overlying strata surface. (a) $H = 0.1$ m; (b) $H = 0.2$ m; (c) $H = 0.3$ m; (d) vertical displacement at different heights after the eighth excavation.

4.2. Deformation Characteristics of the Canal

Deformation of the canal was basically consistent with the rock mass. During the first to seventh excavations, no obvious deformation characteristics were observed. After completion of the eighth excavation, with the overall collapse of the rock mass, obvious deformation and settlement of the channel appeared. Obvious tensile cracks with a width of about 5 mm–10 mm were observed (Figure 8). Thus, the stability of the covered rock directly affected the safe operation of the channel.



Figure 8. Tensile cracks. (a) Overall settlement of cracks in channel dykes; (b) canal crack.

During the test, the channel deformation was monitored by a displacement meter, and the vertical deformation process of different parts of the channel was recorded. During the test, the channel settlement deformation was divided into three stages, namely, the initial deformation stage, deceleration deformation stage, and stability stage. In the initial deformation stage, instability deformation occurred, resulting in maximum settlement deformation; after the initial stage, the settlement deformation of the channel reached equilibrium again and the channel became stabilized, as shown in Figures 9–11. The error of the displacement was less than 0.01 mm.

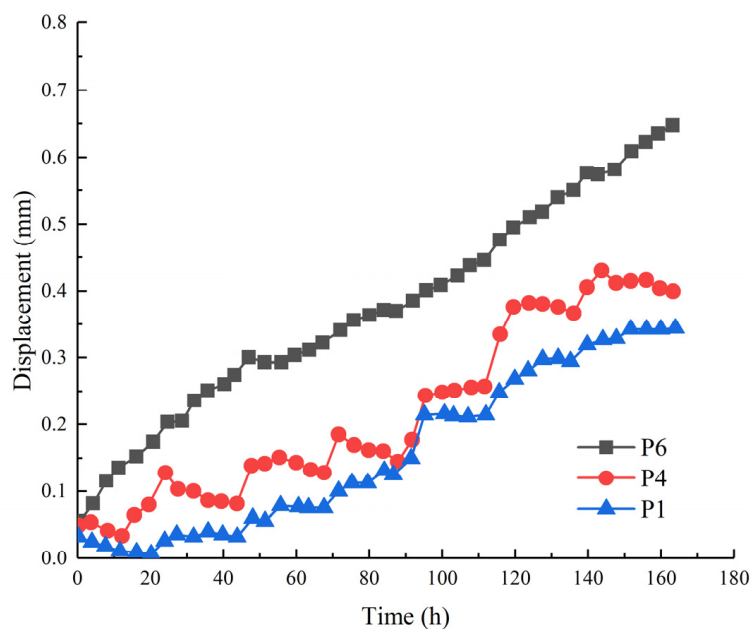


Figure 9. Vertical displacement before failure of observation points P1, P4, and P6.

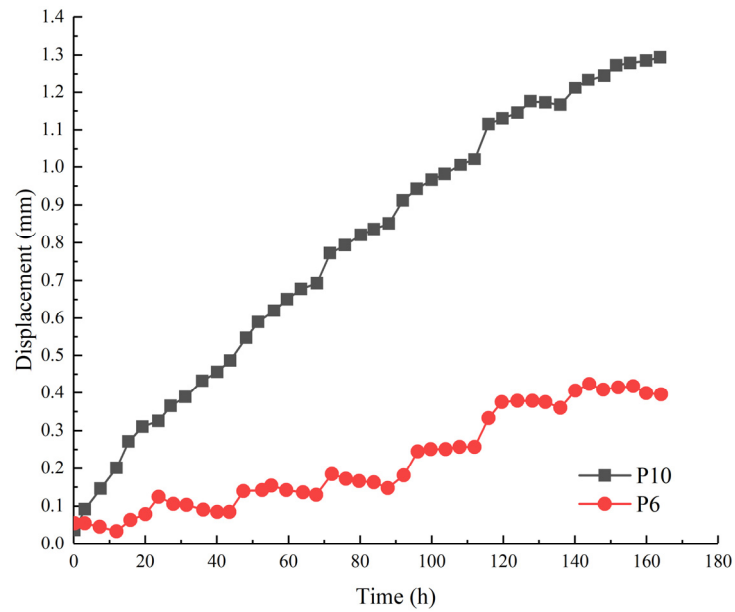


Figure 10. Vertical displacement before failure of observation points P6 and P10.

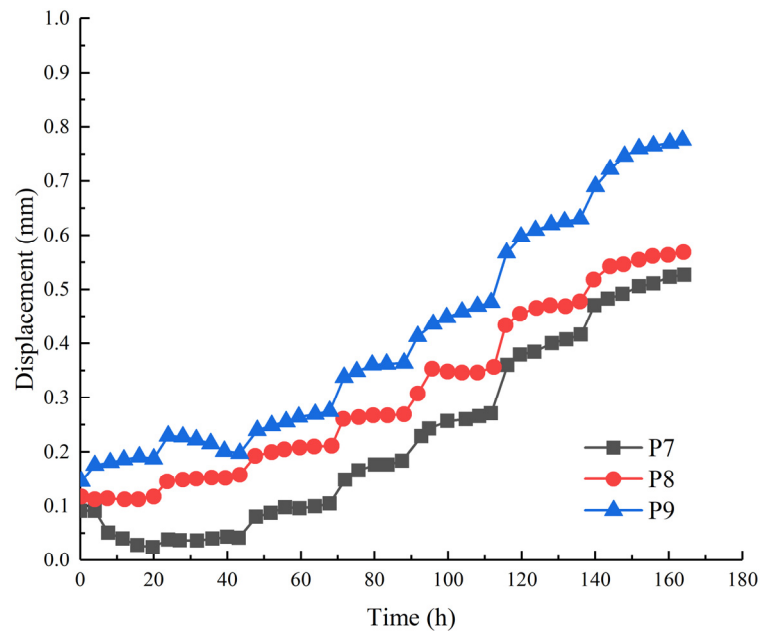


Figure 11. Vertical displacement before failure of observation points P7, P8, and P9.

During the first to the seventh excavations, the vertical settlement deformation of the channel was not large; the deformation amount was between 0 and 1.4 mm, and the maximum vertical deformation appeared on the left side of the channel, which was closest to the top surface of the goaf area. The overall channel was relatively stable. The deformation curve of the observation points at different positions at the same depth of the channel was also analyzed. Before the destruction of the channel, the deformation amount was obviously affected by the distance from the center of the channel: the closer the deformation was to the center, the smaller the vertical deformation from the center (Figure 9).

After the eighth excavation, with the sudden collapse of rock mass and channel subsidence collapse, the maximum settlement of 22 mm appeared at the channel center. For the monitoring points at the same depth on the right side of the channel, the closer they were to the channel center, the higher the vertical deformation value observed. The

collapse area of the channel and embankment was “V”-shaped. The maximum subsidence was observed at the center of the channel, and settlement deformation on both sides of the channel was basically the same. The greater the mining depth, the smaller the deformation, and the smaller the mining depth, the greater the deformation. The excavation of the goaf led to the collapse of the channel, which brought a serious threat to the normal operation of the channel.

5. Discussion and Conclusions

In this paper, the overlying rock body and channel of the goaf in the Yuzhou section of the South-to-North Water Diversion Main Line were taken as the research object, and on the basis of the analysis of geological characteristics, a physical model was established and model tests were carried out to simulate the construction process of underground engineering in the goaf, analyze the deformation and destruction characteristics of the overlying rock body and the vertical deformation characteristics of the channel caused by excavation of the goaf, and establish the critical height ratio as an important discriminant index for overburdened rock bodies and channel collapse in the goaf in the mining area. The following conclusions were drawn.

After excavation construction, the rock mass gradually appeared in the form of horizontal cracks, and the crack length and width increased with the excavation footage. Then, bending deformation and layered collapse were observed in the middle of the goaf. When excavation was conducted to a certain footage, overall collapse and “three-belt” distribution characteristics were observed. Due to the influence of rock collapse, the channel also appeared to experience uneven settlement deformation. The vertical deformation of the channel went through three stages, namely, the initial deformation stage, deceleration deformation stage, and stability stage.

Before the overall collapse of the overlying rock body, channel settlement deformation was very small. The vertical deformation decreased from the channel to the embankment. When the overall collapse occurred, the tension in the center of the channel increased suddenly, and soil on both sides of the channel collapsed toward the center of the channel, presenting “V” glyph collapse. The settlement in the center of the channel measured 22 mm, and there were multiple tensile cracks on both sides of the embankment with widths of 5–10 mm, among which the width of the crack on the left side of the channel was larger: the maximum width on the left side was 10 mm, and the maximum width on the right side was 7 mm.

According to the test process, the vertical deformation and stability of the covered rock was affected by the coal seam recovery process. Before the collapse of the overlying rock body, the vertical deformation was small, and when the goaf was excavated to 76 cm, the overlying rock body suddenly collapsed as a whole, and the channel collapsed and was destroyed, indicating that in the excavation process, there was a critical span ratio R : when $R > 0.039$, the covered rock collapse only occurred within a certain range, whereas when $R < 0.039$, collapse occurred in the covered rock. Controlling the height-to-span ratio of excavation will be the key to ensuring safe construction and channel operation.

However, there is still room for improvement in the research methods of this paper; for example, the selection of model test conditions was relatively simple, and the factors taken into consideration were not comprehensive enough. In addition, the impact of leakage on the safe operation of the channel after the channel is opened to water was not considered. Therefore, in the future, we can continue to carry out relevant research work in combination with the above situation, and the deformation and destruction characteristics of the overlying rock body and the vertical deformation characteristics of the channel can be more accurately analyzed.

Author Contributions: Conceptualization, R.D., H.L. and D.L.; methodology, R.D., Y.T. and D.L.; software, Y.T.; validation, R.D.; formal analysis, Y.T. and D.L.; investigation, R.D., H.L., T.J., H.Y. and D.L.; resources, R.D. and H.L.; data curation, Y.T. and D.L.; writing—original draft preparation, R.D., Y.T. and D.L.; writing—review and editing, Y.T. and D.L.; visualization, Y.T. and D.L.; supervision, H.L., T.J. and H.Y.; project administration, R.D., H.L., T.J. and H.Y.; funding acquisition, R.D. All authors have read and agreed to the published version of the manuscript.

Funding: This research was funded by the National Key R & D Projects (NO. 2019YFC1509704); National Natural Science Foundation of China (NO. U1704243); The Project of High level talents in North China University of Water Resource and Electric Power (NO. 202010013); and Postgraduate Education Reform and Quality Improvement Project of Henan Province (YJS2022JD02, YJS2022AL006).

Institutional Review Board Statement: Not applicable.

Informed Consent Statement: Not applicable.

Data Availability Statement: All data included in this study are available upon request by contacting the corresponding author.

Conflicts of Interest: The authors declare no conflicts of interest.

References

1. Chai, J.; Ouyang, Y.; Liu, J.; Zhang, D.; Du, W.; Lei, W. Experimental study on a new method to forecasting goaf pressure based key strata deformation detected using optic fiber sensors. *Opt. Fiber Technol.* **2021**, *67*, 102706. [[CrossRef](#)]
2. Guo, S.; Guo, G.; Li, H.; Yang, X. Goaf-collapse sites stability evaluation based on principal component hierarchical clustering model. *Chin. J. Geol. Hazard Control* **2020**, *31*, 116–121.
3. Lucha, P.; Cardona, F.; Gutiérrez, F.; Guerrero, J. Natural and human-induced dissolution and subsidence processes in the salt outcrop of the Cardona Diapir (NE Spain). *Environ. Geol.* **2008**, *53*, 1023–1035. [[CrossRef](#)]
4. Ma, G.W.; Hao, H.; Wang, F. Simulations of explosion-induced damage to underground rock chambers. *J. Rock Mech. Geotech. Eng.* **2011**, *3*, 19–29. [[CrossRef](#)]
5. Ma, H.; Wang, J.; Wang, Y. Study on mechanics and domino effect of large-scale goaf cave-in. *Saf. Sci.* **2012**, *50*, 689–694. [[CrossRef](#)]
6. Nazarov, L.A.; Nazarova, L.A. Estimate of the interchamber pillar stability based on the damage accumulation criterion. *J. Min. Sci.* **2007**, *43*, 575–584. [[CrossRef](#)]
7. Tan, Y.; Liu, X.; Ning, J.; Lu, Y. In Situ Investigations on Failure Evolution of Overlying Strata Induced by Mining Multiple Coal Seams. *Geotech. Test. J.* **2017**, *40*, 20160090. [[CrossRef](#)]
8. Wang, Y.; Zheng, G.; Wang, X. Development and application of a goaf-safety monitoring system using multi-sensor information fusion. *Tunn. Undergr. Space Technol.* **2019**, *94*, 103112. [[CrossRef](#)]
9. Xiao, C.; Zheng, H.; Hou, X.; Zhang, X. A stability study of goaf based on mechanical properties degradation of rock caused by rheological and disturbing loads. *Int. J. Min. Sci. Technol.* **2015**, *25*, 741–747. [[CrossRef](#)]
10. Zhang, B.; Zhang, L.; Yang, H.; Zhang, Z.; Tao, J. Subsidence prediction and susceptibility zonation for collapse above goaf with thick alluvial cover: A case study of the Yongcheng coalfield, Henan Province, China. *Bull. Eng. Geol. Environ.* **2016**, *75*, 1117–1132. [[CrossRef](#)]
11. Zhang, C.; Zhao, Y.; Bai, Q. 3D DEM method for compaction and breakage characteristics simulation of broken rock mass in goaf. *Acta Geotech.* **2021**, *17*, 2765–2781. [[CrossRef](#)]
12. Liu, Y.; Li, W.; He, J.; Liu, S.; Cai, L.; Cheng, G. Application of Brillouin optical time domain reflectometry to dynamic monitoring of overburden deformation and failure caused by underground mining. *Int. J. Rock Mech. Min. Sci.* **2018**, *106*, 133–143. [[CrossRef](#)]
13. Castellanza, R.; Gerolymatou, E.; Nova, R. An Attempt to Predict the Failure Time of Abandoned Mine Pillars. *Rock Mech. Rock Eng.* **2007**, *41*, 377. [[CrossRef](#)]
14. Auvray, C.; Homand, F.; Hoxha, D. The influence of relative humidity on the rate of convergence in an underground gypsum mine. *Int. J. Rock Mech. Min. Sci.* **2008**, *45*, 1454–1468. [[CrossRef](#)]
15. Wang, J.A.; Shang, X.C.; Ma, H.T. Investigation of catastrophic ground collapse in Xingtai gypsum mines in China. *Int. J. Rock Mech. Min. Sci.* **2008**, *45*, 1480–1499. [[CrossRef](#)]
16. Han, C.-l.; Zhang, N.; Ran, Z.; Gao, R.; Yang, H.-q. Superposed disturbance mechanism of sequential overlying strata collapse for gob-side entry retaining and corresponding control strategies. *J. Cent. South Univ.* **2018**, *25*, 2258–2271. [[CrossRef](#)]
17. Hanson, J.H.; Bittencourt, T.N.; Ingraffea, A.R. Three-dimensional influence coefficient method for cohesive crack simulations. *Eng. Fract. Mech.* **2004**, *71*, 2109–2124. [[CrossRef](#)]

18. Bäckblom, G.; Martin, C.D. Recent experiments in hard rocks to study the excavation response: Implications for the performance of a nuclear waste geological repository. *Tunn. Undergr. Space Technol.* **1999**, *14*, 377–394. [[CrossRef](#)]
19. Zhang, C.Q.; Zhou, H.; Feng, X.T. An Index for Estimating the Stability of Brittle Surrounding Rock Mass: FAI and its Engineering Application. *Rock Mech. Rock Eng.* **2011**, *44*, 401. [[CrossRef](#)]
20. Detournay, E.; St. John, C.M. Design charts for a deep circular tunnel under non-uniform loading. *Rock Mech. Rock Eng.* **1988**, *21*, 119–137. [[CrossRef](#)]
21. Osgoui, R.R.; Oreste, P. Convergence-control approach for rock tunnels reinforced by grouted bolts, using the homogenization concept. *Geotech. Geol. Eng.* **2007**, *25*, 431–440. [[CrossRef](#)]
22. Guo, G.-L.; Zhu, X.-J.; Zha, J.-F.; Wang, Q. Subsidence prediction method based on equivalent mining height theory for solid backfilling mining. *Trans. Nonferrous Met. Soc. China* **2014**, *24*, 3302–3308. [[CrossRef](#)]
23. Renwei, D.; Handong, L.; Guangxiang, Y.; Jinyu, D. Deformation and Subsidence prediction on Surface of Yuzhou mined-out areas along Middle Route Project of South-to-North Water Diversion, China. *Open Geosci.* **2018**, *10*, 834–843. [[CrossRef](#)]
24. Zhang, S.; Jiang, P.; Lu, L.; Wang, S.; Wang, H. Evaluation of Compressive Geophysical Prospecting Method for the Identification of the Abandoned Goaf at the Tengzhou Section of China's Mu Shi Expressway. *Sustainability* **2022**, *14*, 13785. [[CrossRef](#)]

Disclaimer/Publisher's Note: The statements, opinions and data contained in all publications are solely those of the individual author(s) and contributor(s) and not of MDPI and/or the editor(s). MDPI and/or the editor(s) disclaim responsibility for any injury to people or property resulting from any ideas, methods, instructions or products referred to in the content.